

See discussions, stats, and author profiles for this publication at: <https://www.researchgate.net/publication/279064097>

# Deposition from the Atmosphere to Water and Soils with Aerosol Particles and Precipitation

Chapter · October 2010

DOI: 10.1201/b10262-7

CITATIONS

12

READS

1,049

6 authors, including:



**Matthew MacLeod**  
Stockholm University

219 PUBLICATIONS 11,522 CITATIONS

SEE PROFILE



**Christian Götz**  
ENVILAB AG, Switzerland

15 PUBLICATIONS 578 CITATIONS

SEE PROFILE



**Cliff Davidson**  
Syracuse University

234 PUBLICATIONS 9,146 CITATIONS

SEE PROFILE

Some of the authors of this publication are also working on these related projects:



Ugc project [View project](#)



Partitioning and Persistence of Volatile Methylsiloxanes in Aquatic Environments [View project](#)

---

# 6 Deposition from the Atmosphere to Water and Soils with Aerosol Particles and Precipitation

*Matthew MacLeod, Martin Scheringer,  
Christian Götz, Konrad Hungerbühler,  
Cliff I. Davidson, and Thomas M. Holsen*

## CONTENTS

6.1	Introduction .....	104
6.2	The Transport Processes .....	104
6.2.1	Overview of Dry and Wet Deposition Processes .....	104
6.2.2	Methods for Estimating Gas/Particle Partitioning for Organic Chemicals .....	106
6.2.2.1	One-Parameter Correlations .....	107
6.2.2.2	Two-Parameter Correlations .....	109
6.2.2.3	Polyparameter Linear Free Energy Relationships .....	109
6.2.2.4	Summary of Methods for Estimating Gas/Particle Partitioning of Organic Chemicals .....	110
6.3	Transport Theory .....	111
6.3.1	Dry Particle Deposition .....	111
6.3.2	Wet Particle and Wet Gaseous Deposition .....	112
6.3.3	Wet Deposition on Snow .....	114
6.4	Transport Parameters and Correlations .....	116
6.4.1	Dry Particle Deposition .....	116
6.4.2	Wet Particle and Wet Gaseous Deposition .....	121
6.5	Example Calculations .....	122
6.5.1	Gas/Particle Partitioning .....	122
6.5.2	Dry Deposition .....	124
6.5.3	Wet Deposition .....	125
6.5.4	Look-Up Tables for Mass Transfer Coefficients .....	127
6.6	Summary and Conclusion .....	128

Literature Cited .....	131
Further Reading .....	135

## 6.1 INTRODUCTION

Chemical contaminants in the atmosphere can be deposited to surfaces in association with aerosol particles or falling rain and snow. These are advective transport processes, since the chemical moves in association with aerosol particles, raindrops, or snowflakes. This chapter describes methods for estimating chemical fluxes associated with deposition of aerosol particles and precipitation, and provides recommended values for mass transfer coefficients for a range of environmental conditions. In this chapter we do not consider transport of gaseous species in the atmosphere and adjacent surfaces. These convective transport processes, termed dry deposition of gases, are covered in Chapter 2, Section 2.5.6 and Chapter 7, Section 7.3. exchange between air and plants in Chapter 7, air and water in Chapter 9, and air and snow in Chapter 18.

The deposition processes described in this chapter can be separated into two categories: dry and wet. *Dry deposition* refers to chemical deposited to the surface in association with depositing particles. Here, we deal primarily with deposition to “flat” surfaces with low surface roughness, such as bare soils and water. Chemical transport from the atmosphere to plants and within the canopy is covered in Chapter 7. Particle dry deposition velocities to vegetation may be considerably higher than deposition to flat surfaces. *Wet deposition* refers to chemical deposited to the surface in association with rain or snow. Rain and snow scavenge both particle-associated and gas-phase pollutants, thus we can further differentiate *wet particle deposition* and *wet gaseous deposition*. By their nature, wet deposition processes are episodic.

In this chapter, we first provide a qualitative description of the processes of wet and dry deposition. Since the rates of these processes are controlled to a large extent by the partitioning of contaminants between the gas phase and aerosols in the atmosphere, we review some common methods for estimating the relevant partition coefficient. We then present theory and data to support quantitative modeling of dry deposition, wet deposition during continuous rain, and wet deposition assuming episodic rain events within a steady-state model. We briefly address differences between wet deposition with snow as distinct from rain. Finally, we present a summary of recommended ranges of mass transfer coefficients to describe these processes, and present example calculations for hypothetical chemical property ranges that are representative of the universe of chemicals.

## 6.2 THE TRANSPORT PROCESSES

### 6.2.1 OVERVIEW OF DRY AND WET DEPOSITION PROCESSES

Figure 6.1 illustrates the pathways and partitioning that are components of the dry and wet deposition processes. Ignoring diffusion, a prerequisite for either dry or wet deposition to remove a chemical from the atmosphere is that the chemical must partition to either aerosol particles or falling precipitation. Usually this is described

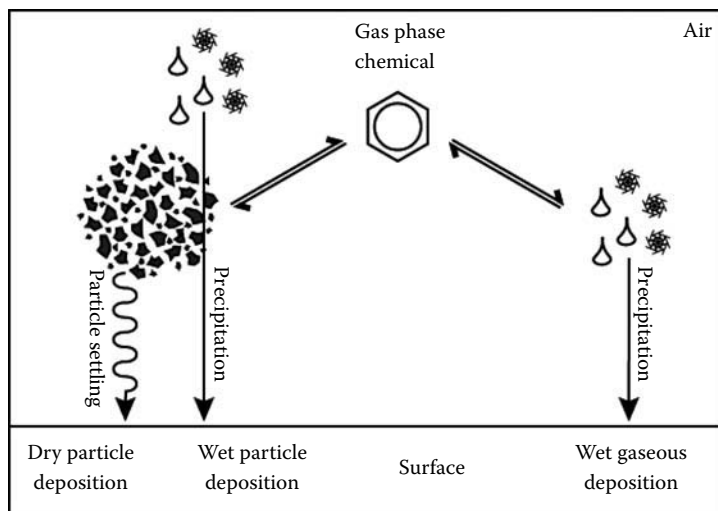


**FIGURE 6.1** Pathways for dry particle deposition, wet particle deposition, and wet gaseous deposition of chemical contaminants from the atmosphere to the surface. Diffusive deposition processes are not dealt with in this chapter, and are not shown.

using a model that assumes equilibrium partitioning between the gas phase and aerosol particles, rain, or snow, indicated in Figure 6.1 by the double-headed arrows. Wet and dry deposition by advection are generally not important processes for volatile chemicals that are virtually entirely in the gas phase at all environmental temperatures.

Rates of both wet deposition and dry particle deposition can be estimated from mass transfer coefficients. The mass transfer coefficient for wet deposition is directly proportional to the rainfall rate ( $r$ , m/h, or equivalently  $\text{m}^3/\text{m}^2/\text{h}$ ). Similarly, the dry deposition velocity of particles ( $U_D$ , m/h) determines the mass transfer coefficient for dry particle deposition. Both  $r$  and  $U_D$  can be converted into equivalent volumetric flow rates since wet deposition and dry particle deposition are advective processes.

Wet gaseous deposition is important for chemicals that are normally present in the gas phase but can be scavenged by rain drops and/or snowflakes, that is, chemicals that have large water–air and/or ice–air partition coefficients. Polar semivolatile chemicals such as many modern pesticides are examples of chemicals that are efficiently removed from the atmosphere by wet gaseous deposition.

Dry particle deposition and wet particle deposition are important processes for pollutants that are strongly associated with aerosols in the atmosphere. For example, heavy metals released from natural and anthropogenic sources are completely associated with aerosol particles in the atmosphere. Organic chemicals with low vapor pressure are also strongly associated with aerosol particles in the atmosphere, and are thus subject to dry and wet particle deposition. Because of the importance of partitioning between aerosols and the gas phase to the process of wet and dry particle deposition, we briefly review estimation methods below.

### 6.2.2 METHODS FOR ESTIMATING GAS/PARTICLE PARTITIONING FOR ORGANIC CHEMICALS

Methods for estimating the degree of sorption of chemicals to aerosols have been reviewed by Bidleman and Harner [1], Wania et al. [2], and Cousins and Mackay [3]. Here we provide a brief summary of methods reviewed by these authors, and some additional details of methods that have emerged since the publication of these reviews.

The distribution of chemicals between the gas phase and aerosol particles has most commonly been quantified by  $K_P$  ( $\text{m}^3 \text{ air}/\mu\text{g aerosol}$ ),

$$K_P = \frac{C_P^*}{C_A}, \quad (6.1)$$

where  $C_P^*$  is the particle-associated concentration ( $\text{mol}/\mu\text{g aerosol}$ ) and  $C_A$  is the gas-phase concentration ( $\text{mol}/\text{m}^3 \text{ air}$ ). The chemical quantity unit ( $\text{mol}$ ) cancels and can be substituted by a mass quantity such as grams or milligrams. Vapor–particle partitioning is usually determined from field studies using a high-volume air sampler equipped with a filter to capture aerosol particles followed in-line by a vapor trap to collect gas-phase chemical. The amount of chemical contaminant captured on the filter and in the vapor trap is determined analytically, and  $K_P$  is calculated as

$$K_P = \frac{\left( \frac{C_F}{\text{TSP}} \right)}{C_A}, \quad (6.2)$$

where  $C_F$  ( $\text{mol}/\text{m}^3 \text{ air}$ ) is the amount of chemical on the filter per unit volume of air, and TSP is the total suspended particle concentration ( $\mu\text{g aerosol}/\text{m}^3 \text{ air}$ ).

It is conceptually important to distinguish between *absorption* of chemical into the bulk particle and *adsorption* of chemical to the surface of the particles. If absorption is the dominant sorption process and the aerosol particles are assumed to be homogeneous, the sorption capacity of aerosol particles is proportional to their volume. In this case,  $K_P$  can be converted directly into a volumetric partition coefficient,  $K_{PA}$  ( $\text{m}^3 \text{ air}/\text{m}^3 \text{ aerosol particles}$ ), with knowledge of the density of aerosol particles ( $\rho_P$ ,  $\text{kg}/\text{m}^3$ )

$$K_{PA} = K_P \rho_P \times 10^9, \quad (6.3)$$

where the factor  $10^9$  converts micrograms of aerosol into kilograms.  $K_{PA}$  is a convenient measure of gas/particle partitioning since it is  $C_P$  ( $\text{mol}/\text{m}^3 \text{ aerosols}$ )/ $C_A$  ( $\text{mol}/\text{m}^3 \text{ air}$ ), and it is thus directly analogous to other volumetric partition coefficients such as  $K_{AW}$  and  $K_{OW}$ . Assuming a density of aerosol particles of  $2000 \text{ kg}/\text{m}^3$  [1,2], Equation 6.3 becomes  $K_{PA} = K_P \times 2 \times 10^{12}$ .

Alternatively, if adsorption dominates total sorption,  $K_P$  is proportional to the total particle surface area and it can be expressed as a surface area-based partition

coefficient,  $K_{SA}$  ( $\text{m}^3 \text{ air}/\text{m}^2$  aerosol particle area):

$$K_{SA} = \frac{K_P \rho_P \times 10^9}{\left(\frac{SA}{V}\right)}, \quad (6.4)$$

where  $SA/V$  is the surface area-to-volume ratio of the aerosol particles ( $\text{m}^2$  particles/ $\text{m}^3$  particles). If we assume aerosol particles to be spherical, the ratio of surface area-to-volume is  $3/r$ , where  $r$  is the particle radius. For an average particle radius of  $2 \mu\text{m}$ ,  $SA/V$  is  $3/2 \times 10^6 \text{ m}^2$  particles/ $\text{m}^3$  particles. Thus, for our generic aerosol, Equation 6.4 becomes  $K_{SA} = K_P \times 4/3 \times 10^6$ .

Despite the important conceptual difference, it is often difficult to distinguish between absorption and adsorption as the dominant mechanism, particularly for data gathered in the field. Therefore it is useful to be able to convert between  $K_{PA}$  and  $K_{SA}$ , which are related by the surface area-to-volume ratio,

$$K_{PA} = \frac{SA}{V} \times K_{SA}. \quad (6.5)$$

Assuming spherical particles with a radius of  $2 \mu\text{m}$ , Equation 6.5 is  $K_{PA} = 3/2 \times 10^6 \times K_{SA}$ . Thus, for a generic aerosol particle scenario,  $K_{PA}$  can be estimated as  $K_P \times 2 \times 10^{12}$  regardless of whether an absorptive or adsorptive mechanism is dominant. And, with knowledge of average particle radius and aerosol particle density,  $K_P$ ,  $K_{PA}$ , and  $K_{SA}$  can be interconverted. For most mass balance modeling applications, the most convenient form is  $K_{PA}$ , and we use it exclusively for the remainder of this chapter.

The fraction of particle-associated chemical in bulk air  $\Phi$ , (dimensionless), can be calculated from  $K_{PA}$  and the volume fraction of aerosol particles in air,

$$\phi = \frac{K_{PA}}{K_{PA} + \frac{V_A}{V_P}}, \quad (6.6)$$

where  $V_A$  and  $V_P$  are the volumes of air and aerosols, respectively.

### 6.2.2.1 One-Parameter Correlations

Pankow proposed two models of vapor/particle partitioning based on surface adsorption [4] and absorption [5]. Both models predict inverse relationships between  $K_{PA}$  and the liquid-state saturation vapor pressure ( $P_L$ , Pa) that have the form [2]:

$$K_{PA} = \frac{x}{P_L}. \quad (6.7)$$

In the adsorption model, the parameter  $x$  is a function of available surface area and the enthalpy of sorption. In the absorption model,  $x$  is proportional to the amount of available organic matter and inversely proportional to the activity coefficient of chemical dissolved in organic matter. Based on data for PAH sorption to urban aerosols,

Mackay [6] has suggested  $x = 6 \times 10^6$  Pa as a reasonable estimate that allows  $K_{PA}$  to be estimated from Equation 6.7.

Finizio et al. [7] provided an alternative interpretation of the Pankow absorption model [5] in terms of the octanol/air partition coefficient ( $K_{OA}$ ,  $\text{m}^3 \text{ air}/\text{m}^3 \text{ octanol}$ )

$$K_{PA} = BK_{OA}. \quad (6.8)$$

The coefficient  $B$  ( $\text{m}^3 \text{ octanol}/\text{m}^3 \text{ aerosol particles}$ ) is directly proportional to the fraction of available organic matter in aerosols ( $f_{OM}$ ), the ratio of densities of aerosol particles and octanol ( $\rho_P/\rho_O$ ), the ratio of molecular weights of octanol and organic matter ( $M_O/M_{OM}$ ), and the ratio of activity coefficients of the chemical in octanol and organic matter ( $\gamma_O/\gamma_{OM}$ ),

$$B = f_{OM} \frac{\rho_P}{\rho_O} \frac{M_O}{M_{OM}} \frac{\gamma_O}{\gamma_{OM}}. \quad (6.9)$$

Bidleman and Harner [1] suggested a generic value of  $B = 0.5$  based on  $\rho_O = 840 \text{ kg}/\text{m}^3$ , and the assumptions that  $f_{OM} = 0.5$ ,  $\rho_P = 2000 \text{ kg}/\text{m}^3$ ,  $(M_O/M_{OM}) = 1$  and  $(\gamma_O/\gamma_{OM}) = 1$ .

Götz et al. [8] reviewed the composition of aerosol particles in different representative environmental scenarios and found that the fine fraction ( $< 2.5 \mu\text{m}$  diameter) has  $f_{OM}$  that is typically 3.5 times higher than the coarse fraction (diameter between 2.5 and  $10 \mu\text{m}$ ). This difference in  $f_{OM}$  is attributable to different sources of the fine and coarse fractions. Götz et al. [8] also recommend  $(M_O/M_{OM}) = 0.26$  based on measurements of the molecular weight of aerosol organic matter by Kalberer et al. [9]. Adopting this recommendation with the other assumptions above implies  $B = 0.13$  is a reasonable generic value that can be used to estimate  $K_{PA}$  from  $K_{OA}$ . Further assuming that the total aerosol volume is equally distributed between the fine and coarse fractions implies  $B$  for the fine fraction is 0.20 and  $B$  for the coarse fraction is 0.057.

Xiao and Wania [10] compared vapor pressure and octanol/air partition coefficient as descriptors of partitioning between air and organic matter. Using a data set for over 200 nonpolar, nonionizing organic chemicals they demonstrated empirically that  $K_{OA}$  and  $P_L$  are approximately inversely proportional to one another,

$$P_L (\text{Pa}) \approx \frac{10^{6.7}}{K_{OA}}. \quad (6.10)$$

They conclude that  $K_{OA}$  and  $P_L$  are both equally well suited for describing partitioning of nonpolar organic chemicals between the gas phase and aerosol organic matter.

By combining Equations 6.7 and 6.10, we observe that assuming  $x = 6 \times 10^6$  in Equation 6.7 is equivalent to assuming  $B = 1.2$  in Equation 6.8. This result is not conceptually satisfying since it implies that bulk aerosols have a sorption capacity for nonpolar organic chemicals that exceeds that of octanol, which is unlikely. We therefore recommend  $x = 6 \times 10^5$  for predicting  $K_{PA}$  from vapor pressure using Equation 6.7, and  $B = 0.13$  for estimating  $K_{PA}$  from  $K_{OA}$  using Equation 6.8. These recommendations should provide estimates of  $K_{PA}$  that are approximately consistent whether they are based on vapor pressures or octanol/air partition coefficients.

### 6.2.2.2 Two-Parameter Correlations

Data from field studies of partitioning of semivolatile chemicals between aerosols and air are often empirically fitted using two-parameter equations based on  $P_L$  or  $K_{OA}$ ,

$$\log K_{PA} = m \log P_L + b, \quad (6.11)$$

$$\log K_{PA} = m' \log K_{OA} + b', \quad (6.12)$$

where  $m$ ,  $m'$ ,  $b$ , and  $b'$  are fitting parameters specific to the set of data under consideration. Equation 6.11 is equivalent to the one-parameter approach (Equation 6.7) when  $m = -1$  and  $b = \log x$ . Likewise, when  $m' = 1$  and  $b' = \log B$ , Equation 6.12 reduces to the one-parameter Equation 6.8. Bidleman and Harner [1] provide a summary table of regressions of  $\log K_P$  versus  $\log P_L$  from field studies, and Xiao and Wania [10] provide references to studies using both  $P_L$  and  $K_{OA}$ . Generally, the absolute value of  $m$  and  $m'$  determined from field studies ranges between 0.6 and 1.

### 6.2.2.3 Polyparameter Linear Free Energy Relationships

In a critical review of gas/solid and gas/liquid partitioning of organic chemicals, Goss and Schwarzenbach [11] call attention to the potential for error in applying one- or two-parameter correlations to predict gas/particle partitioning. A one-parameter correlation with  $P_L$  assumes that activity coefficients of all sorbates in aerosol particles are equal and a one-parameter correlation with  $K_{OA}$  assumes that organic matter absorption is the dominant sorption process in aerosols and that the ratio of sorbate activities in octanol and aerosol organic matter are equal for all possible sorbates. However, compound-specific interactions between the sorbate molecules and aerosols can render these assumptions invalid, and this is especially possible for chemicals with polar functional groups. Deviations from these assumptions lead to slopes in Equations 6.11 and 6.12 with absolute values different from 1, and would imply errors in the one-parameter correlations. In addition, Goss and Schwarzenbach [11] point out that two-parameter correlations are only strictly valid within a group of structurally related substances because of the potential for different types of specific interactions to apply for different compound classes.

As an alternative, Goss and coworkers have advocated modeling partitioning between the gas phase and aerosol particles using polyparameter linear free energy relationships (pp-LFERs) [12]. A pp-LFER for absorption into the bulk particle phase has the general form

$$\log K_{PA} = a_{\text{bulk}} \log K_{HXA} + b_{\text{bulk}} \Sigma\beta + c_{\text{bulk}} \Sigma\alpha + d_{\text{bulk}} V_m + \text{const}_{\text{bulk}}. \quad (6.13)$$

Each of the multiplicative terms in Equation 6.13 conceptually represents a type of possible interaction between the chemical and the aerosol particle bulk phase. These are van der Waals interactions ( $a_{\text{bulk}} \log K_{HXA}$ ), electron donor–acceptor interactions ( $b_{\text{bulk}} \Sigma\beta$  and  $c_{\text{bulk}} \Sigma\alpha$ ) and cavity formation in the sorbent ( $d_{\text{bulk}} V_m$ ). The constant,  $\text{const}_{\text{bulk}}$ , depends on the dimensions of  $\log K_{PA}$ .  $\log K_{HXA}$  is the decadic logarithm of the hexadecane/air partition coefficient,  $\Sigma\beta$  and  $\Sigma\alpha$  are chemical descriptors that characterize electron donor and electron acceptor ability, and  $V_m$  is the




McGowan molar volume of the chemical. These four chemical properties are examples of Abraham chemical descriptors, which are named after Michael Abraham, who pioneered this approach [13]. The parameters  $a_{\text{bulk}}$ ,  $b_{\text{bulk}}$ ,  $c_{\text{bulk}}$ , and  $d_{\text{bulk}}$  are empirically derived descriptors that are properties of the aerosol under consideration. These aerosol property descriptors are temperature-dependent and also dependent on relative humidity when adsorption is the dominant sorption mechanism. Polyparameter linear free energy relationships have been developed to describe absorptive partitioning between air and bulk aerosol particles [14,15], as well as adsorption to aerosol components such as mineral surfaces and salts [16,17] and to snow [18].

Götz et al. [8] compared a gas/particle partitioning model based on the pp-LFER approach with the  $K_{\text{OA}}$  approach with the goal of defining the limits of applicability of the  $K_{\text{OA}}$  model. They concluded that for nonpolar chemicals and cases where sorption is dominated by absorption into organic matter, the two model approaches are highly correlated and either is appropriate. However, for polar chemicals sorbing to low-organic matter aerosols at low humidity, such as in arctic or desert regions, the two approaches differed by up to several orders of magnitude and the pp-LFER approach is preferable.

### 6.2.2.4 Summary of Methods for Estimating Gas/Particle Partitioning of Organic Chemicals

Table 6.1 summarizes recommended methods for estimating the dimensionless aerosol particle/air partition coefficient,  $K_{\text{PA}}$ , from vapor pressure,  $K_{\text{OA}}$  or using pp-LFERs.

**TABLE 6.1**  
**Recommended Methods for Estimating  $K_{\text{PA}}$**

		<b>One-Parameter Correlations</b>
$K_{\text{PA}} = 6 \times 10^{-5} / P_{\text{L}} \text{ (Pa)}$		Screening-level estimation of partitioning of polar and nonpolar substances in generic evaluative environments.
$K_{\text{PA}} = 0.13 K_{\text{OA}}$		
Fine fraction $K_{\text{PA}} = 0.20 K_{\text{OA}}$		
Coarse fraction $K_{\text{PA}} = 0.057 K_{\text{OA}}$		
		<b>Two-Parameter Correlations</b>
$\log K_{\text{PA}} = m \log P_{\text{L}} + b$		Calculation of site-specific partitioning of polar and nonpolar substances where absorption by organic matter dominates. Fitting parameters can be applied within a substance class.
$\log K_{\text{PA}} = m' \log K_{\text{OA}} + b'$		
		<b>Polyparameter Linear Free Energy Relationships</b>
$\log K_{\text{PA}} = a_{\text{bulk}} \log K_{\text{HXA}} + b_{\text{bulk}} \Sigma\beta$ $+ c_{\text{bulk}} \Sigma\alpha + d_{\text{bulk}} V_{\text{m}}$ $+ \text{const}_{\text{bulk}}$		General calculation of site-specific partitioning for polar and nonpolar substances and absorptive or adsorptive mechanisms.

### 6.3 TRANSPORT THEORY

A detailed and comprehensive theoretical description of dry particle deposition and wet deposition processes can be found in Seinfeld and Pandis [19], and treatments with a specific focus on trace contaminants are provided in the texts by Mackay [6], Thibodeaux [20], and Scheringer [21]. In this section, we review this transport theory and place special emphasis on a method to approximate the effect of intermittent rainfall events in a steady-state model.

#### 6.3.1 DRY PARTICLE DEPOSITION

The flux of dry particle-associated chemical from the atmosphere to the surface ( $N_D$ , mol/h) can be calculated from the estimated dry deposition velocity of particles ( $U_D$ , m/h);

$$N_D = U_D A C_P V_P / V_A, \quad (6.14)$$

where  $A$  ( $\text{m}^2$ ) is the horizontal area that receives the deposition,  $C_P$  ( $\text{mol}/\text{m}^3$  particles) is the concentration of chemical in aerosol particles and  $V_P/V_A$  is the volume fraction of particles in air. In general cases it is more convenient to calculate  $N_D$  from the total chemical concentration in bulk air,  $C_B$ , where  $C_B = C_A + C_P V_P/V_A$ . Then,

$$N_D = U_D \phi A C_B. \quad (6.15)$$

The group  $U_D \phi$  can be interpreted as a chemical- and environment-specific mass transfer coefficient for dry particle deposition,  $k_D$  (m/h).

Selecting accurate and representative estimates of  $U_D$  is a challenge because it bundles several competing processes. Figure 6.2 illustrates a conceptual resistance model for dry deposition of small and large particles. Small, low-density particles are mixed in the atmosphere like gases and do not fall under the influence of gravity. For these particles,  $U_D$  can be calculated as

$$U_D = \frac{1}{1/k_A + 1/k_B}, \quad (6.16)$$

where  $k_A$  (m/h) is the mass transfer coefficient for aerodynamic transport in the constant flux layer and  $k_B$  (m/h) is the mass transfer coefficient for transport through the stagnant air layer above the depositional surface by random Brownian motion. At a given time and location,  $k_A$  and  $k_B$  are determined by wind speed, atmospheric stability, and roughness height of the depositional surface. Windy conditions and a rough depositional surface increase  $k_A$  and  $k_B$  and thus increase  $U_D$  of small particles [19]. Additional information about  $k_A$  and  $k_B$  are presented in Chapter 7, where they are referred to as their reciprocal resistances ( $R_A = 1/k_A$  and  $R_B = 1/k_B$ ). For large and dense aerosol particles, dry deposition under the influence of gravity dominates and  $U_D$  is approximately equal to the gravitational settling velocity of particles through viscous air ( $U_S$ , m/h) [19].

In this chapter, we focus on deposition to surfaces with low surface roughness, such as bare soils and water. Dry deposition of fine particles to grassland or forested

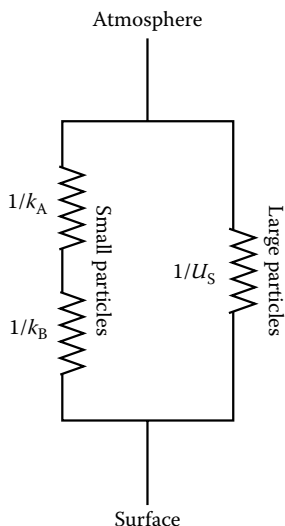


**FIGURE 6.2** Conceptual resistance model of resistances that control the rate of dry particle deposition.

areas can be much higher because of the high surface roughness of the receiving surface, and is discussed in Chapter 7.

### 6.3.2 WET PARTICLE AND WET GASEOUS DEPOSITION

Chemical flux due to wet particle deposition ( $N_{WP}$ , mol/h) can be calculated as

$$N_{WP} = U_R Q A C_P V_P / V_A, \quad (6.17)$$

where  $U_R$  is the rain rate (m/h) and  $Q$  (dimensionless) is the scavenging ratio, representing the volume of air that is efficiently scavenged of aerosol particles by a unit volume of rain. This can also be expressed in terms of the total concentration in bulk air,  $C_B$ ,

$$N_{WP} = U_R Q \phi A C_B. \quad (6.18)$$

The group  $U_R Q \phi$  in Equation 6.18 can be interpreted as a chemical- and environment-specific mass transfer coefficient for wet particle deposition,  $k_{WP}$  (m/h).

Wet gaseous deposition ( $N_{WG}$ , mol/h) can be calculated as

$$N_{WG} = U_R A C_R, \quad (6.19)$$

where  $C_R$  (mol/m<sup>3</sup> rain) is the concentration of chemical in falling rain. Assuming that immediately after rain starts the gas-phase concentration of chemical ( $C_A$ , mol/m<sup>3</sup> air) becomes distributed between the gas phase and raindrops, we obtain

$$C_A V_A = C_{A,R} V_A + C_R V_R, \quad (6.20)$$

where  $C_{A,R}$  (mol/m<sup>3</sup> air) is the concentration in the gas phase during rainfall. Rearranging Equation 6.20 yields

$$\frac{C_A}{C_R} = \frac{C_{A,R}}{C_R} + \frac{V_R}{V_A}. \quad (6.21)$$

If we assume equilibrium partitioning between the gas phase and raindrops during the rain event,  $C_{A,R}/C_R = K_{AW}$ , and

$$C_R = \frac{C_A}{K_{AW} + \frac{V_R}{V_A}} = \frac{C_B(1 - \phi)}{K_{AW} + \frac{V_R}{V_A}}. \quad (6.22)$$

Thus the concentration in rain and the wet gaseous deposition flux is dependent on  $K_{AW}$  and the volume fraction of raindrops in air during rainfall [22]. The term  $V_R/V_A$  in Equation 6.22 acts as a limit on the chemical concentration that can develop in raindrops for very hydrophilic substances with very low  $K_{AW}$ . It has a typical value of  $6 \times 10^{-8}$  m<sup>3</sup> water/m<sup>3</sup> air [22]. This term has often been omitted from calculations of wet gaseous deposition [6,21], which leads to overestimation of  $C_R$  and  $N_{WG}$  for hydrophilic compounds with log  $K_{AW}$  less than  $\sim 7.5$ .

Equation 6.19 can be expressed in terms of total concentration in bulk air as

$$N_{WG} = \frac{U_R(1 - \phi)}{K_{AW} + \frac{V_R}{V_A}} AC_B. \quad (6.23)$$

Thus the group  $(U_R(1 - \phi))/(K_{AW} + V_R/V_A)$  in Equation 6.23 can be interpreted as a chemical- and environment-specific mass transfer coefficient for wet gaseous deposition,  $k_{WG}$  (m/h).

The equations above are formulated to calculate time-averaged wet particle and wet gaseous deposition flux over several rain events. This approach is particularly useful for calculating steady-state solutions to mass balance chemical fate models, since the time-variant rate of deposition with rainfall is represented as a continuous process, that is, the model assumes a constant light drizzle of rain. However, the effects of intermittent rain events on average chemical concentrations in air over several rain events are not well described for all chemicals by assuming constant rainfall [22,23].

Jolliet and Hauschild [22] point out that the intermittent nature of rainfall events imposes a limit on the timescale that chemicals can be removed from the atmosphere by wet particle and wet gaseous deposition. Consider a hypothetical chemical that is efficiently removed from the atmosphere by rain. Figure 6.3 illustrates the atmospheric residence time due to wet deposition for such a chemical over a rainfall cycle that includes a dry period of duration  $t_{dry}$  and a wet period of duration  $t_{wet}$ . If the chemical is released to the atmosphere immediately following the end of a rain event, its residence time in the atmosphere is  $t_{dry}$ . If it is released during a rain event, its residence time is approximately zero. The average atmospheric residence time for a chemical released during the dry period is  $t_{dry}/2$ . Over the long term,

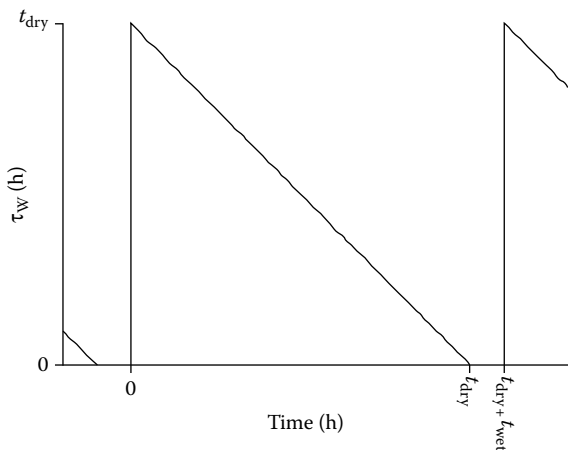


**FIGURE 6.3** Atmospheric residence time due to wet deposition processes of a hypothetical chemical that is efficiently removed from the atmosphere by rainfall ( $\tau_W$ , h) during a rain event cycle including a dry period ( $t_{\text{dry}}$ ) and a wet period ( $t_{\text{wet}}$ ).

the average atmospheric residence time over several cycles of dry and wet periods,  $\bar{\tau}_{W,\text{MIN}}$  (h), is

$$\bar{\tau}_{W,\text{MIN}} = \frac{t_{\text{dry}}}{2} \times \frac{t_{\text{dry}}}{t_{\text{dry}} + t_{\text{wet}}}. \quad (6.24)$$

The subscript “MIN” denotes that  $\bar{\tau}_{W,\text{MIN}}$  is the minimum possible long-term average atmospheric residence time due to wet deposition processes for chemicals that are efficiently scavenged by rain. The maximum possible long-term average flux of chemical to the surface due to wet deposition processes is

$$N_{W,\text{MAX}} = \frac{2(t_{\text{dry}} + t_{\text{wet}})}{t_{\text{dry}}^2} h A C_B, \quad (6.25)$$

where  $h$  (m) is the mixing height of the atmosphere, which is typically set at 1000 m, representing the planetary boundary layer. The term  $2h(t_{\text{dry}} + t_{\text{wet}})/t_{\text{dry}}^2$  can be interpreted as an environment-specific maximum limit on the total mass transfer coefficient for wet deposition ( $k_{W,\text{MAX}}$ , m/h). When the group  $(k_{WP} + k_{WG})$ , is calculated assuming continuous rain, is greater than  $k_{W,\text{MAX}}$ ,  $k_{W,\text{MAX}}$  should be used to estimate the time-averaged wet deposition flux over several rain events.

### 6.3.3 WET DEPOSITION ON SNOW

If the temperature is below 0°C, snow instead of rain causes “wet” deposition of chemicals. Like rain, snow is an advective process that transfers both gaseous and particle-bound chemicals from the air to the ground, and it is desirable to be able to estimate the mass transfer coefficients for these processes. The most important

factors determining the rate of wet deposition by snow are the snow–air partition coefficient of the chemical [18], the specific surface area of the snowflakes [24], and temperature, which influences both the snow–air partition coefficient and the specific surface area [25,26].

The mechanism of sorption of chemicals to snow is different from their dissolution in rain droplets. Equilibrium partitioning between the gas phase and snowflakes can be described using a partition coefficient between snow surface and air,  $K_{SA}$ . Recently, Roth et al. [18] have measured  $K_{SA}$  to snow for a set of 57 organic chemicals and derived the following pp-LFER describing sorption of organic chemicals:

$$\log K_{SA}(-6.8^{\circ}\text{C}) = 0.639 \cdot \log K_{HXA} + 3.53 \cdot \sum \alpha + 3.38 \cdot \sum \beta - 6.85. \quad (6.26)$$

As described above in Section 6.2.2,  $K_{SA}$  has units of  $\text{m}^3 \text{ air}/\text{m}^2 \text{ snow surface}$ . The volumetric snowflake–air partition coefficient,  $K_{FA}$  ( $\text{m}^3 \text{ air}/\text{m}^3 \text{ snow}$ ) is analogous to  $K_{PA}$ , and can be obtained from Equation 6.5, where the surface area-to-volume ratio of snow is calculated as the product of the specific surface area of the snowflakes ( $SSA_F$  in  $\text{m}^2 \text{ snow surface}/\text{kg snow}$ ), and the density of the snowflakes ( $\rho_F$ , in  $\text{kg snow}/\text{m}^3 \text{ snow}$ ). Typical values for  $SSA_F$  and  $\rho_F$  are  $100 \text{ m}^2/\text{kg}$  [24] and  $920 \text{ kg}/\text{m}^3$ .

It is important to note that the extent of partitioning to snowflakes is temperature-dependent and will be higher at lower temperatures. Goss and Schwarzenbach [27], and Roth et al. [28] describe methods for estimating the temperature dependence of partitioning to snow.

From the snowflake–air partition coefficient ( $K_{FA}$ ) and the precipitation rate for snow,  $U_F$  (m/h), the chemical flux due to wet deposition with snowflakes can be derived:

$$N_{WG,F} = \frac{U_F(1 - \phi)}{(K_{FA})^{-1} + \frac{V_F}{V_A}} \cdot AC_B, \quad (6.27)$$

where  $V_F/V_A$  is the volume fraction of snowflakes in air during a snowfall event. The group  $(U_F(1 - \phi))/((K_{FA})^{-1} + V_F/V_A)$  in Equation 6.27 can be interpreted as a chemical- and environment-specific mass transfer coefficient for wet gaseous deposition on snowflakes,  $k_{WG,F}$  (m/h).

Wet gaseous deposition by snow can be very efficient if the temperature is low. In particular, large molecules with a high affinity to snow because of high  $\Sigma\beta$  values, such as  $\alpha$ -HCH, are efficiently deposited with falling snow. Compounds with very low vapor, pressure such as high molecular weight PAHs and decabromodiphenylether, have high  $K_{FA}$  but also have high octanol–air partition coefficients, and are therefore mainly bound to atmospheric aerosol particles [25,26].

Wet particle deposition by snow can be calculated using an equation analogous to Equation 6.18,

$$N_{WP,F} = U_F Q \phi AC_B. \quad (6.28)$$

As a first approximation, the same scavenging ratio ( $Q$ ) can be assumed to apply to both snow as rain in generic models.

## 6.4 TRANSPORT PARAMETERS AND CORRELATIONS

### 6.4.1 DRY PARTICLE DEPOSITION

Figure 6.4 summarizes the range of possible particle dry deposition velocities ( $U_D$ ) as a function of particle diameter (the gray area and the primary vertical axis). This figure is adapted from information presented in Seinfeld and Pandis [19] on deposition velocity determined in a wind tunnel and on generic aerosol distributions. The range of  $U_D$  shown in gray in Figure 6.4 corresponds approximately to surface roughness heights in the range 0.1–3 cm and particle densities between 1000 and 4000 kg/m<sup>3</sup>.

Generally speaking, the uncertainty range for particles smaller than 0.02–0.03  $\mu\text{m}$  is a factor of  $10\times$  whereas for larger particles it is a factor of  $5\times$ . So, it is evident from Figure 6.4 that any generic, single value selected for  $U_D$  will be subject to large uncertainties due to variability in particle size, surface roughness, and particle density. Table 6.2 summarizes recommended values for  $f_{OM}$  and  $V_P/V_A$  for different environmental scenarios, based on data presented in Figure 6.4. The value for the generic aerosol scenario is from Bidleman and Harner [1], and values for other scenarios are estimated from data presented by Putaud et al. [29] and Götz et al. [8].

It is of interest to ask what deposition velocities might exist for smooth, flat surfaces, such as soil or water surfaces, or artificial surfaces such as asphalt, under a range of wind conditions. Such values may be useful in defining lower limits to deposition from the ambient atmosphere. Measurements and models for dry deposition to rougher surfaces such as vegetation are discussed in Chapter 7.

For particles with diameter greater than several micrometers in light winds, deposition to smooth surfaces will be dominated by gravity; values of the sedimentation velocity  $U_S$  for particles of various sizes depositing under the influence of gravity are given by Seinfeld and Pandis [19]. For particles smaller than this size range, or for particles depositing to smooth, flat surfaces in strong winds, turbulent inertial deposition will increase the deposition velocity.

Data on particle deposition to smooth surfaces were obtained in the wind tunnel experiments by Sehmel [30] and Sehmel and Hodgson [31] for a wide range of particle sizes. For example, Figure 6.5 shows  $U_D$  versus particle diameter  $d_p$  for a roughness height of 0.001 cm at friction velocities of 720 m/h (light winds) and 3600 m/h (strong winds) for unit density particles. The line corresponding to the sedimentation velocity is also shown for comparison. Note that the curve for 720 m/h joins the sedimentation line for  $d_p$  greater than about 15  $\mu\text{m}$ . The curve for 3600 m/h joins the sedimentation line for  $d_p$  greater than about 60  $\mu\text{m}$ .

Figure 6.5 can be used with size distributions of chemical species from the literature to estimate a lower limit to the dry deposition velocity for that species on rougher natural surfaces. If the molar airborne concentration of a chemical in size range  $i$  is given by  $C_{Pi}$  (mol/m<sup>3</sup> particles) and the volume fraction of particles of size range  $i$  in air is given by  $V_{Pi}/V_A$ , then the overall average deposition velocity  $U_{D\text{--average}}$  is given by

$$U_{D\text{--average}} = \frac{\sum_{i=1}^n U_{Di} C_{Pi} \frac{V_{Pi}}{V_A}}{\sum_{i=1}^n C_{Pi} \frac{V_{Pi}}{V_A}}. \quad (6.29)$$

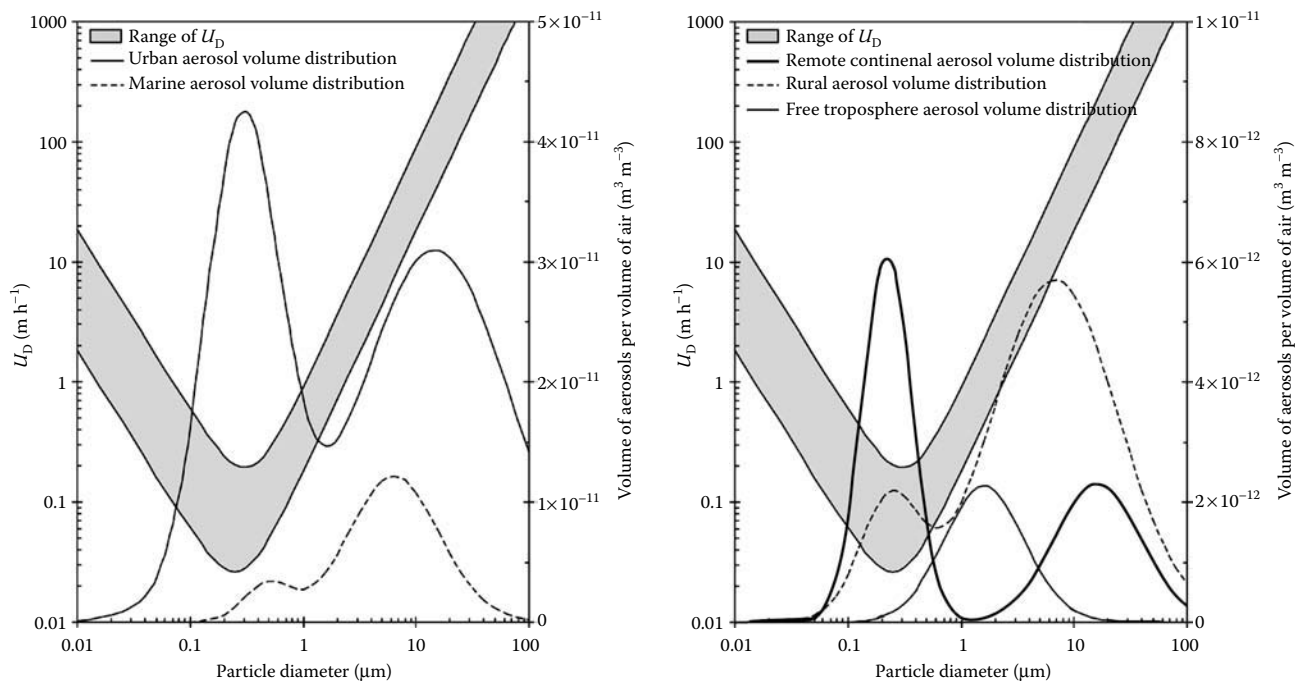


**FIGURE 6.4** Particle dry deposition velocity ( $U_D$ , primary vertical axis) as a function of particle diameter compared with representative volume distributions of aerosol particles (secondary vertical axis).



**TABLE 6.2**  
**Recommended Values of Aerosol Particle Volume Fraction in Air ( $V_p/V_A$ , dimensionless) and Volume Fraction of Organic Matter in Aerosols ( $f_{OM}$ , dimensionless) for Different Environmental Scenarios**

Aerosol Scenario		$U_D$ (m/h)	$V_p/V_A$	$f_{OM}$
Generic		4.6	$2 \times 10^{-11}$	0.5
Free troposphere		1	$2 \times 10^{-11}$	0.2
Urban	Fine fraction	0.2	$4 \times 10^{-10}$	0.3
	Coarse fraction	20	$5 \times 10^{-10}$	0.1
Rural	Fine fraction	0.2	$2 \times 10^{-11}$	0.3
	Coarse fraction	20	$8 \times 10^{-11}$	0.1
Remote continental	Fine fraction	0.2	$4 \times 10^{-11}$	0.3
	Coarse fraction	20	$2 \times 10^{-11}$	0.1
Marine	Fine fraction	0.2	$2 \times 10^{-11}$	0.1
	Coarse fraction	10	$1 \times 10^{-10}$	0.05

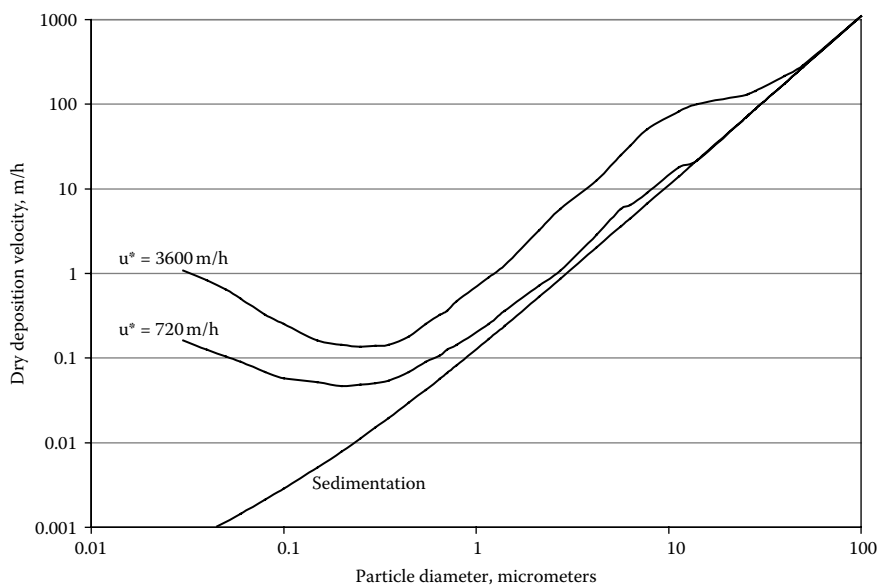


**FIGURE 6.5** Dry deposition velocity of unit-density particles on a smooth, flat surface at friction velocities of  $u^* = 720$  m/h and 3600 m/h. The line for sedimentation by gravity is also shown for comparison. Calculations for this graph are taken from the model of Sehmel and Hodgson [31].

**TABLE 6.3**  
**Calculated Dry Deposition Velocities for a Smooth, Flat Surface**  
**Based on Size Distribution Data in the Literature for Pb, Mn, and Ca**

Metal	N	Average Diameter (μm)	Geom. Mean Concentration (ng/m <sup>3</sup> )	<i>U<sub>D</sub></i> –ave (m/h)	
Pb	41	0.55	310	3.5	Sedimentation
				3.6	<i>u</i> * = 720 m/h
				12	<i>u</i> * = 3600 m/h
Mn	32	2.06	20	7.9	Sedimentation
				8.3	<i>u</i> * = 720 m/h
				24	<i>u</i> * = 3600 m/h
Ca	20	4.64	330	13	Sedimentation
				15	<i>u</i> * = 720 m/h
				41	<i>u</i> * = 3600 m/h

We have used size distribution data from the review of Milford and Davidson [32] for three trace metals with Equation 6.29 to calculate  $U_{D\text{--average}}$  for these metals. Results are shown in Table 6.3. Note that  $N$  refers to the number of separate size distributions reported in the literature for each metal. Pb is primarily submicron, and is known to be a result of anthropogenic combustion processes including use of leaded gasoline, metallurgical processing, coal combustion, and numerous other sources. The small values of  $U_{D\text{--average}}$  reflect the relatively small particle sizes associated with Pb. Note that  $U_{D\text{--average}}$  is only slightly greater for a friction velocity of 720 m/h compared with sedimentation due to weak turbulent inertial deposition on the surface. However, the value of  $U_{D\text{--average}}$  is considerably greater for a friction velocity of 3600 m/h due to much greater turbulent delivery to the surface that accompanies higher wind speeds.

The original calculations show that most of the mass flux of Pb is due to those particles in the uppermost size ranges. Milford and Davidson [32] assumed a maximum aerodynamic diameter of 40 μm; the estimated values of  $U_{D\text{--average}}$  are sensitive to this assumed maximum.

Mn is a trace metal of intermediate sizes, with particles that originate both from anthropogenic and natural sources. The greater values of  $U_{D\text{--average}}$  compared with Pb reflect the larger particle sizes.

Ca is mainly derived from the Earth’s crust, with airborne particles resulting mainly from abrasion of rock and soil. The particle sizes of Ca are much larger than either Pb or Mn, and the deposition velocities are correspondingly greater. Table 6.4 summarizes typical  $U_{D\text{--average}}$  values. Curves of  $U_D$  versus particle diameter for a smooth surface can be used as a rough estimate of deposition to a calm water surface as long as wave action is negligible. For a lake or ocean surface with significant waves, particle deposition will be enhanced. This is due to increased air turbulence from the wave motion as well as greater inertial impaction as particles are captured by the wave. Zufall et al. [33] have modeled waves with a variety of ratios of  $2a/\lambda$  where

**TABLE 6.4**  
**Typical Overall Deposition Velocities**

Pollutant	Overall $U_D$ , m/h (Typical Range)	Comments	References
$\text{SO}_4^{2-}$	3–100		[37–39]
$\text{NO}_3^-$	3–70		[37,38,40]
$\text{NH}_4^+$	3–70		[37]
$\text{Cl}^-$	40–200		[37]
Primarily crustal metals (Al, Ca, Mg, K...)	40–100	Nonurban	[37,41–45]
	70–400	Urban	[37,42–45]
Primarily anthropogenic metals (Pb, Cu, Zn, Ni, Cd...)	3–40	Nonurban	[37,42–45]
	40–250	Urban	[37,42–45]
Particle associated semivolatile organics (PCBs, PAHs...)	3–70	Nonurban	[42,46–49]
	20–200	Urban	[46,49–53]
TSP	20–200	Nonurban	[40]
	40–400	Urban	[40]

$2a$  = peak-to-trough amplitude and  $\lambda$  = length of the wave. For  $2a/\lambda = 0.03$ , deposition of  $1\text{ }\mu\text{m}$  diameter particles is enhanced by a factor of 50% over the corresponding deposition to a smooth, flat surface. For  $2a/\lambda = 0.01$ , deposition is enhanced by a factor of 100%.

If the particles are hygroscopic, deposition to a water surface may also be enhanced by particle growth in the humid boundary layer just over the surface. For example, ammonium sulfate particles will grow by water uptake and thus have a greater deposition velocity compared with nonhygroscopic particles. However, particle transport through the humid boundary layer may be faster than hygroscopic growth so that the effects of growth are limited.

Ammonium sulfate particles are normally dry crystalline solids as relative humidity increases up to a value of about 80%. If the humidity exceeds that value, the particle will uptake water and grow, transitioning from a solid to a solution droplet. But if humidity then falls below 80%, the droplet will not dry out but rather exist as a supersaturated solution as long as the humidity stays above 36%. Liquid droplets existing in such a supersaturated state are *metastable*, and such particles behave differently than particles that have never deliquesced even though they are identical in all other respects.

Figure 6.6 shows a graph of  $U_D$  versus particle diameter  $d_p$  for ammonium sulfate for several conditions. Curve A refers to the hypothetical case where there is no uptake of water and therefore no increase in  $U_D$ . This is the base case. Curve B shows the maximum increase in deposition velocity that can be expected, if hygroscopic growth

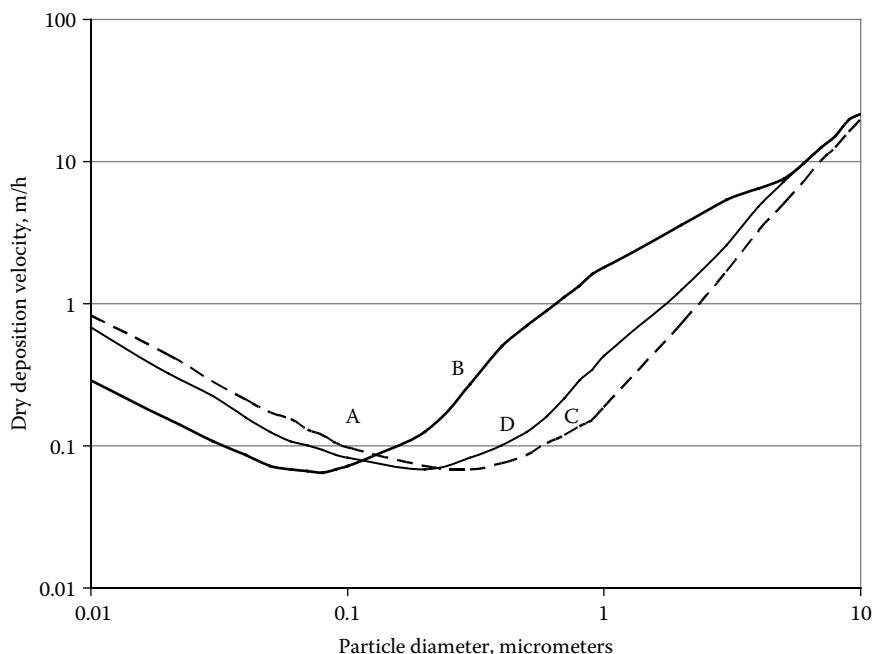


**FIGURE 6.6** Dry deposition velocity of ammonium sulfate particles to a smooth water surface for a windspeed of 2 m/s,  $T = 20^\circ\text{C}$ , relative humidity at 1 m = 75%, and initial particle height = 1 m. Curve A is the baseline case without any hygroscopic growth, while Curve B is for growth to equilibrium. Curve C is for partial growth of metastable liquid particles. Curve D is for partial growth of particles that deliquesce from solid crystals to become liquid. [Adapted from Zufall, M.J. et al., *Environ. Sci. Technol.*, 1998, **32**(5), 584–590.]

is so rapid that the particle reaches equilibrium well within the humidity boundary layer. Curve C shows the deposition velocity for metastable particles that are still in a solution phase. These particles have much slower growth since they are already in a liquid state; a realistic humidity profile has been taken from Avery [34]. Finally, Curve D shows ammonium sulfate particles that deliquesce from a solid crystalline form to a liquid droplet taking into account the humidity profile.

The large values of  $U_D$  for the equilibrium case in this figure, say for  $1\ \mu\text{m}$ , compared with the cases that account for time needed for growth suggest that one cannot assume equilibrium has been achieved. Rather it is important to account for timescales of growth when dealing with hygroscopic particles. The third and fourth curves are probably the most realistic when estimating ammonium sulfate deposition to an ambient water surface.

#### 6.4.2 WET PARTICLE AND WET GASEOUS DEPOSITION

The long-term global average precipitation rate ( $U_R$ ) is  $9.7 \times 10^{-5}$  m/h, equivalent to 0.85 m/year, and this value has been recommended as a generic value for chemical fate modeling [6,21]. However, rain rate is highly variable geographically and seasonally,

**TABLE 6.5**

**Recommended Generic Yearly Average Values of Rain Rate ( $U_R$ , m/h), Time between Rain Events ( $t_{dry}$ , h) and Duration of Rain Events ( $t_{wet}$ , h) for Selected Environmental Scenarios**

Environmental Scenarios	$U_R$		$t_{dry}$ (h)	$t_{wet}$ (h)
	(m/h)	(m/year)		
Generic global average	$9.7 \times 10^{-5}$	0.85	120	12
Desert	$1 \times 10^{-6}$	$8.8 \times 10^{-3}$	720	12
Continental	$1 \times 10^{-4}$	0.88	120	12
Tropical	$3 \times 10^{-4}$	2.6	48	12

therefore locally relevant data should be used whenever possible. The International Research Institute for Climate and Society at Columbia University provides historical precipitation rate and precipitation frequency ( $t_{dry}$ ) data through their Web site, <http://iri.ldeo.columbia.edu/>. We have compiled a selection of these data in Table 6.5 as recommended values for generic regional assessments. In the absence of data for a specific location, we recommend assuming that the interval between rain events ( $t_{dry}$ ) is 5 days (120 h) and that the duration of rain events ( $t_{wet}$ ) is 12 h [22]. Using these generic values the minimum possible long-term average atmospheric residence time due to wet deposition processes ( $\bar{\tau}_{W,MIN}$ , see Equation 6.24) is 55 h.

A scavenging ratio ( $Q$ ) of  $2 \times 10^5$  is recommended by Mackay [6] as a typical generic value. This corresponds to a 1 mm<sup>3</sup> raindrop falling from a height of 200 m and intercepting all particles in its path, or falling from 1000 m and intercepting 20% of particles. Table 6.6 summarizes measured values of  $Q$  found in the literature. Seinfeld and Pandis [19] review factors that control the collision efficiency between raindrops and aerosol particles. By analogy to dry deposition, large aerosol particles are efficiently collected by falling raindrops by inertial impaction and small aerosol particles are efficiently collected as a result of Brownian diffusion into the raindrop. However, particles in the 0.1–1  $\mu\text{m}$  size range are too large to have appreciable Brownian diffusivity, and too small to be efficiently collected by impaction.

## 6.5 EXAMPLE CALCULATIONS

Below we present sample calculations of the important parameters discussed in this chapter for selected organic chemicals with different properties and nickel, which is representative of involatile substances that have no vapor pressure. The chemical property data used in this section are all taken from the handbook of Mackay et al. [35].

### 6.5.1 GAS/PARTICLE PARTITIONING

- Given that the logarithm of the octanol–air partition coefficient ( $\log K_{OA}$ ) of benzene is 2.78, estimate the volumetric gas–particle partition coefficient ( $K_{PA}$ ) and the fraction associated with aerosols ( $\phi$ ) under typical generic environmental conditions.

TABLE 6.6  
Typical Values of Scavenging Ratio, *Q*

Pollutant	Scavenging Ratios, Volume Basis (m/V) <sub>rain</sub> /(m/V) <sub>air</sub> ,	Comments	References
	Typical range or value <sup>a</sup>		
SO <sub>4</sub> <sup>2-</sup>	0.1–17	Rain	[54–56]
	0.02–6	Snow	[55,56]
NO <sub>3</sub> <sup>-</sup>	0.3–1.4	Rain	[54]
	1–3	Snow	[56]
		(total nitrate)	
NH <sub>4</sub> <sup>+</sup>	0.1–3	Rain	[56]
	1	Snow	[56]
Primarily crustal metals (Al, Ca, Mg, Mn, K ...)	0.1–4.5	Rain	[54,57]
Primarily anthropogenic metals (Pb, Cu, Zn, Ni, Cd ...)	0.02–0.5	Rain	[54,55,57]
Particle associated semivolatile organics (PCBs, PAHs ...)	0.001–0.6	Rain	[47,54,57,58]
	0.1–50	Snow	[58,59]
Gas-associated semivolatile organics (PCBs, PAHs ...)	0.01–1	Rain	[54,59]
	0.01–0.3	Snow	[58]
Total PCBs (gas + particle)	0.001–2	Rain	[55,58,60]
	0.05–10	Snow	[55,58]
Total PAHs (gas + particle)	0.001–300	Rain	[55,58]
	0.01–50	Snow	[55,58]

<sup>a</sup> Values have been multiplied by 10<sup>-6</sup>.

Using Equation 6.8 and the constant recommended by Götz et al. [8],  $K_{PA} = 0.13K_{OA}$ . The octanol–air partition coefficient of benzene is  $10^{2.78} = 600$ , therefore,  $K_{PA}$  for benzene is  $78 \text{ m}^3 \text{ air/m}^3 \text{ aerosol particles}$ .

Using Equation 6.6 and assuming the volume fraction of aerosols in air is  $2 \times 10^{-11} \text{ m}^3 \text{ aerosol particles/m}^3 \text{ air}$  (Table 6.2),  $\phi = K_{PA}/(K_{PA} + 2 \times 10^{11})$ . Substituting  $K_{PA} = 78 \text{ m}^3 \text{ air/m}^3 \text{ aerosol particles}$  for benzene,  $\phi = 3.9 \times 10^{-10}$  which is approximately zero. Therefore, benzene is expected to be virtually entirely in the gas phase in the atmosphere.

- b. Calculate  $K_{PA}$  and  $\phi$  from  $\log K_{OA}$  for hexachlorobenzene (HCB), Lindane, benzo(a)pyrene (B(a)P), and nickel using the same assumptions.

Results are summarized below in Table 6.7. Note that since nickel has a negligible vapor pressure it does not partition to air and  $K_{OA}$  and  $K_{PA}$  are essentially infinite.

**TABLE 6.7**

**Log Octanol/Air Partition Coefficient ( $\log K_{OA}$ ) and Calculated Volumetric Particle/Air Partition Coefficient ( $K_{PA}$ ) and Fraction Associated with Aerosol Particles ( $\phi$ ) under a Generic Scenario for Five Example Chemicals**

Substance	$\log K_{OA}$	$K_{PA}$	$\phi$
Benzene	2.78	78	$3.9 \times 10^{-10}$
Hexachlorobenzene	6.78	$7.8 \times 10^5$	$3.9 \times 10^{-6}$
Lindane	7.92	$1.1 \times 10^7$	$5.4 \times 10^{-5}$
Benzo(a)pyrene	10.77	$7.7 \times 10^9$	0.037
Nickel	(Large)	(Large)	1

From the form of Equation 6.6 it is clear that  $\phi$  will be low for chemicals that have  $K_{PA}$  lower than  $V_A/V_P$ , which has a typical value of about  $2 \times 10^{11}$ . Benzene, HCB, and Lindane all have very low  $\phi$  and can be expected to be found predominantly in the gas phase under most environmental conditions. B(a)P is estimated to be 4% on particles under this generic scenario, and  $\phi$  may be considerably higher at low temperatures, or when aerosol particle concentrations are higher, for example in an urban area. Nickel can be expected to be 100% particle-associated in the atmosphere under all conditions.

### 6.5.2 DRY DEPOSITION

- Calculate the mass transfer coefficient for dry deposition ( $k_D$ , m/h) of benzene, HCB, Lindane, B(a)P, and nickel for the generic environmental scenario, then calculate the time required for half of the bulk atmospheric burden of each chemical to be removed by dry deposition.

From Equation 6.15,  $k_D = U_D \phi$ . For the generic scenario,  $U_D = 4.6$  m/h (Table 6.2). Using this value along with  $\phi$  of  $3.9 \times 10^{-10}$  for benzene, we calculate  $k_D$  for benzene as  $1.8 \times 10^{-9}$  m/h, and  $k_D$  for the other four substances as HCB:  $1.8 \times 10^{-5}$  m/h, Lindane:  $2.5 \times 10^{-4}$  m/h, B(a)P: 0.17 m/h, and nickel: 4.6 m/h. The half time for removal of a chemical from the atmosphere by dry deposition is  $(\ln 2 \times h/k_D)$  where  $h$  is the mixing height of the atmosphere and is assumed to be 1000 m, representing the planetary boundary layer. Substituting values for  $k_D$  for each chemical yields the following times for half of the atmospheric burden to be removed by dry deposition; benzene:  $3.9 \times 10^{11}$  h, or about 44 million years; HCB:  $3.9 \times 10^7$  h, or about 4 thousand years; Lindane:  $2.8 \times 10^6$  h or about 320 years; B(a)P:  $4.1 \times 10^3$  h or about 6 months; nickel:  $1.5 \times 10^2$  h, or about 1 week.

It is apparent from these calculations that dry deposition is not a very efficient process in the generic scenario except for chemicals that are highly sorbed to aerosols. However, it can be important under specific conditions, especially when chemicals

**TABLE 6.8**  
**Equations and Parameter Values for Calculating Wet Deposition**  
**for the Example Chemicals**

Process	Equation	Parameter Values
Wet particle deposition	$k_{WP} = U_R Q \phi$	$U_R = 9.7 \times 10^{-5} \text{ m/h}$
Wet gaseous deposition	$k_{WG} = \frac{U_R(1 - \phi)}{(K_{AW} + V_R/V_A)}$	$Q = 5 \times 10^4$ $V_R/V_A = 6 \times 10^{-8}$
Maximum wet deposition mass transfer coefficient	$k_{W,MAX} = \frac{2h(t_{dry} + t_{wet})}{t_{dry}^2}$	$h = 1000 \text{ m}$ $t_{dry} = 120 \text{ h}$ $t_{wet} = 12 \text{ h}$

are associated with coarse particles, or in cases where the receiving surface has a high roughness height and is efficient at scavenging fine particles.

### 6.5.3 WET DEPOSITION

Given the air/water partition coefficient ( $K_{AW}$ ), calculate mass transfer coefficients and half-times for removal by wet particle and wet gaseous deposition of the example chemicals for a generic environmental scenario assuming constant drizzling rain. Compare the sum of these mass transfer coefficients to the maximum possible long-term average mass transfer coefficient for wet deposition given the intermittent nature of rainfall.

Equations and generic environmental parameters required to calculate the mass transfer coefficients for wet deposition are summarized from the text in Table 6.8.

Table 6.9 provides the logarithm of the air–water partition coefficient for each example chemical and values for the calculated mass transfer coefficients for wet deposition in units of m/h.

**TABLE 6.9**  
**Logarithm of the Air/Water Partition Coefficient ( $\log K_{AW}$ ) for the**  
**Example Chemicals and Mass Transfer Coefficients for Wet Deposition**  
**in Units of m/h**

Substance	$\log K_{AW}$	$k_{WP}$	$k_{WG}$	$k_{WP} + k_{WG}$	$k_{W,MAX}$
Benzene	−0.65	$1.9 \times 10^{-9}$	$4.3 \times 10^{-4}$	$4.3 \times 10^{-4}$	18.3
Hexachlorobenzene	−1.28	$1.9 \times 10^{-5}$	$1.9 \times 10^{-3}$	$1.9 \times 10^{-3}$	18.3
Lindane	−4.22	$2.6 \times 10^{-4}$	1.6	1.6	18.3
Benzo(a)pyrene	−4.73	0.18	5	5.2	18.3
Nickel	n/a	4.9	0	4.9	18.3



As shown in Table 6.9,  $(k_{WP} + k_{WG})$  is less than  $k_{W,MAX}$  for all of the example chemicals. Therefore, the continuous rain assumption is not producing unrealistically high wet deposition rates for these chemicals. The half-times for total wet deposition of the substances are benzene,  $1.6 \times 10^6$  h or about 180 years; HCB,  $3.7 \times 10^5$  h or about 40 years; Lindane, 431 h or 18 days; B(a)P, 134 h or 5.6 days; and nickel, 143 h or 6 days. Benzene and HCB are not efficiently removed from the atmosphere by wet deposition. Lindane and B(a)P are removed by wet gaseous deposition, and nickel by wet particle deposition. The 6-day half-life of nickel in the atmosphere represents the half-life for removal of particles by wet deposition in the generic scenario. This value is sensitive to the selected values for the rain rate and the scavenging ratio. The value of the maximum mass transfer coefficient for wet deposition corresponds to a minimum half-life in air of 38 h or 1.6 days.

**TABLE 6.10**  
**Fraction of Particle-Associated Chemical in the Atmosphere ( $\phi$ )**

		log $K_{OW}$									
		-1	0	1	2	3	4	5	6	7	8
log $K_{AW}$	2	0	0	0	0	0	0	0	0	0	0
	1	0	0	0	0	0	0	0	0	0	0
	0	0	0	0	0	0	0	0	0	0	0
	-1	0	0	0	0	0	0	0	0	0	0
	-2	0	0	0	0	0	0	0	0	0	0.03
	-3	0	0	0	0	0	0	0	0	0.03	0.21
	-4	0	0	0	0	0	0	0	0.03	0.21	0.72
	-5	0	0	0	0	0	0	0.03	0.21	0.72	0.96
	-6	0	0	0	0	0	0.03	0.21	0.72	0.96	1.00
	-7	0	0	0	0	0.03	0.21	0.72	0.96	1.00	1.00
	-8	0	0	0	0.03	0.21	0.72	0.96	1.00	1.00	1.00
	-9	0	0	0.03	0.21	0.72	0.96	1.00	1.00	1.00	1.00
	-10	0	0.03	0.21	0.72	0.96	1.00	1.00	1.00	1.00	1.00
	-11	0.03	0.21	0.72	0.96	1.00	1.00	1.00	1.00	1.00	1.00

Note:  $\Phi$  calculated as a function of log  $K_{OW}$  and log  $K_{AW}$  using Equation 6.6 and assuming  $K_{PA} = 0.13 K_{OA}$  and  $V_P/V_A = 2 \times 10^{-11}$ .

6.5.4 LOOK-UP TABLES FOR MASS TRANSFER COEFFICIENTS

The mass transfer coefficients described in this chapter are functions of chemical partitioning properties and environmental conditions. For nonionizing organic chemicals, the range of possible partitioning in the environment can be represented by octanol–water partition coefficients between  $10^{-1}$  and  $10^8$  and air–water partition coefficients between  $10^{-11}$  and  $10^2$  [36]. To a first approximation,  $K_{OA} = K_{OW}/K_{AW}$ , thus the relevant range of partitioning encompasses a range of  $K_{OA}$  from  $10^{19}$  to  $10^{-1}$ .

Tables 6.10 through 6.15 contain results for example calculations of  $\Phi$  and the mass transfer coefficients  $k_D$ ,  $k_{WP}$ , and  $k_{WG}$  calculated using our recommended values for a generic environmental scenario for the range of plausible partitioning properties of organic chemicals defined above. Also included is a look-up table for  $k_{W,TOT}$ .

TABLE 6.11  
Mass Transfer Coefficient for Dry Particle Deposition ( $K_D$ , m/h)

		log $K_{OW}$									
		-1	0	1	2	3	4	5	6	7	8
log $K_{AW}$	2	0	0	0	0	0	0	0	0	0	0
	1	0	0	0	0	0	0	0	0	0	0
	0	0	0	0	0	0	0	0	0	0	0
	-1	0	0	0	0	0	0	0	0	0	0.01
	-2	0	0	0	0	0	0	0	0	0.01	0.12
	-3	0	0	0	0	0	0	0	0.01	0.12	0.95
	-4	0	0	0	0	0	0	0.01	0.12	0.95	3.32
	-5	0	0	0	0	0	0.01	0.12	0.95	3.32	4.43
	-6	0	0	0	0	0.01	0.12	0.95	3.32	4.43	4.58
	-7	0	0	0	0.01	0.12	0.95	3.32	4.43	4.58	4.60
	-8	0	0	0.01	0.12	0.95	3.32	4.43	4.58	4.60	4.60
	-9	0	0.01	0.12	0.95	3.32	4.43	4.58	4.60	4.60	4.60
	-10	0.01	0.12	0.95	3.32	4.43	4.58	4.60	4.60	4.60	4.60
	-11	0.12	0.95	3.32	4.43	4.58	4.60	4.60	4.60	4.60	4.60

Note: Calculated as  $U_D\phi$ , assuming  $U_D = 4.6$  m/h.

**TABLE 6.12**  
**Mass Transfer Coefficient for Wet Particle Deposition ( $k_{WP}$ , m/h)**

		log $K_{OW}$									
log $K_{AW}$		-1	0	1	2	3	4	5	6	7	8
	2	0	0	0	0	0	0	0	0	0	0
	1	0	0	0	0	0	0	0	0	0	0
	0	0	0	0	0	0	0	0	0	0	0
	-1	0	0	0	0	0	0	0	0	0	0.01
	-2	0	0	0	0	0	0	0	0	0.01	0.12
	-3	0	0	0	0	0	0	0	0.01	0.12	1.00
	-4	0	0	0	0	0	0	0.01	0.12	1.00	3.50
	-5	0	0	0	0	0	0.01	0.12	1.00	3.50	4.67
	-6	0	0	0	0	0.01	0.12	1.00	3.50	4.67	4.83
	-7	0	0	0	0.01	0.12	1.00	3.50	4.67	4.83	4.85
	-8	0	0	0.01	0.12	1.00	3.50	4.67	4.83	4.85	4.85
	-9	0	0.01	0.12	1.00	3.50	4.67	4.83	4.85	4.85	4.85
	-10	0.01	0.12	1.00	3.50	4.67	4.83	4.85	4.85	4.85	4.85
	-11	0.12	1.00	3.50	4.67	4.83	4.85	4.85	4.85	4.85	4.85

*Note:* Calculated as  $U_R Q \phi$ , where  $\phi$  is from Table 6.10 and assuming  $U_R = 9.7 \times 10^{-5}$  m/h and  $Q = 5 \times 10^4$ .

which represents the total mass transfer coefficient for wet deposition considering the maximum possible rate due to the intermittent nature of rainfall events, and for  $k_{TOT}$ , the total mass transfer coefficient for all aerosol-associated deposition processes simultaneously. Values calculated above for the example chemicals can be cross checked in the look-up tables using the log  $K_{AW}$  values in Table 6.9 and the following log  $K_{OW}$  values: benzene, 2.13; HCB, 5.50; Lindane: 3.70; B(a)P, 6.04; nickel, large.

6.6 SUMMARY AND CONCLUSION

In this chapter we have reviewed the theory of dry particle and wet deposition of chemical contaminants from the atmosphere to surfaces, and we have provided

**TABLE 6.13**  
**Mass Transfer Coefficient for Wet Gaseous Deposition ( $k_{WG}$ , m/h)**

		log $K_{OW}$									
log $K_{AW}$		-1	0	1	2	3	4	5	6	7	8
	2	0	0	0	0	0	0	0	0	0	0
	1	0	0	0	0	0	0	0	0	0	0
	0	0	0	0	0	0	0	0	0	0	0
	-1	0	0	0	0	0	0	0	0	0	0
	-2	0.01	0.01	0.01	0.01	0.01	0.01	0.01	0.01	0.01	0.01
	-3	0.10	0.10	0.10	0.10	0.10	0.10	0.10	0.10	0.09	0.08
	-4	0.97	0.97	0.97	0.97	0.97	0.97	0.97	0.94	0.77	0.27
	-5	9.64	9.64	9.64	9.64	9.64	9.62	9.40	7.65	2.68	0.36
	-6	91.5	91.5	91.5	91.5	91.3	89.2	72.6	25.4	3.39	0.35
	-7	606	606	606	605	591	481	168	22.5	2.32	0.23
	-8	1386	1385	1382	1351	1100	385	51.3	5.31	0.53	0.05

*Note:* Calculated as  $(U_R(1 - \phi)/K_{AW} + V_R/V_A)$ , where  $\phi$  is from Table 6.10 and assuming  $U_R = 9.7 \times 10^{-5}$  m/h and  $V_R/V_A = 6 \times 10^{-8}$  m<sup>3</sup> water/m<sup>3</sup> air.

recommended values to estimate rates of deposition under generic environmental scenarios. Accurately estimating the rates of these processes is a considerable challenge because they depend on both (1) the extent of partitioning of chemical between the gas phase and aerosol particles or precipitation and (2) the rate of deposition of the aerosol particles and precipitation. We stress that there is considerable uncertainty in estimation equations to describe gas–particle partitioning, and in estimates of dry deposition velocities and scavenging ratios. In addition, there is a high degree of variability in aerosol size distribution and composition, which impacts both partitioning and deposition velocities.

Considering these uncertainties and variability, it is clear that estimates of the rates of dry particle and wet deposition based on the generic parameters suggested here

**TABLE 6.14**  
**Total Maximum Mass Transfer Coefficient for Wet**  
**Gaseous Deposition ( $k_{W,TOT}$ , m/h)**

		log $K_{OW}$									
log $K_{AW}$		-1	0	1	2	3	4	5	6	7	8
	2	0	0	0	0	0	0	0	0	0	0
	1	0	0	0	0	0	0	0	0	0	0
	0	0	0	0	0	0	0	0	0	0	0
	-1	0	0	0	0	0	0	0	0	0	0.01
	-2	0.01	0.01	0.01	0.01	0.01	0.01	0.01	0.01	0.02	0.13
	-3	0.10	0.10	0.10	0.10	0.10	0.10	0.10	0.11	0.22	1.08
	-4	0.97	0.97	0.97	0.97	0.97	0.97	0.98	1.07	1.77	3.77
	-5	9.64	9.64	9.64	9.64	9.64	9.63	9.52	8.65	6.18	5.03
	-6	18.3	18.3	18.3	18.3	18.3	18.3	18.3	18.3	8.06	5.18
	-7	18.3	18.3	18.3	18.3	18.3	18.3	18.3	18.3	7.15	5.08
	-8	18.3	18.3	18.3	18.3	18.3	18.3	18.3	10.1	5.38	4.90
	-9	18.3	18.3	18.3	18.3	18.3	18.3	10.9	5.46	4.91	4.86
	-10	18.3	18.3	18.3	18.3	18.3	11.0	5.47	4.91	4.86	4.85
	-11	18.3	18.3	18.3	18.3	11.0	5.47	4.91	4.86	4.85	4.85

*Note:* Calculated as the minimum of ( $k_{WP} + k_{WG}$ ) from Tables 6.11 and 6.12 and  $2h(t_{dry} + t_{wet})/t_{dry}^2$ , assuming  $h = 1000$  m,  $t_{dry} = 120$  h, and  $t_{wet} = 12$  h.

could easily be in error by an order of magnitude or more when compared to measurements from field studies. Site- and event-specific data or regression equations should be used in preference to generic values to estimate the rates of dry particle and wet deposition whenever data are available. Experimental work in several areas is desirable to further evaluate and refine the models and parameter values recommended here. First, more measurements of gas-particle partitioning of organic chemicals in a variety of different aerosols under laboratory or field conditions are needed. Experiments that determine the concentration and composition of the aerosol in addition to the chemical concentrations in the gas phase and on particles are particularly valuable; however, this type of study has only rarely been conducted. Second,

**TABLE 6.15**  
**Total Mass Transfer Coefficient for Dry and Wet**  
**Deposition ( $k_{TOT}$ , m/h)**

		log $K_{OW}$									
log $K_{AW}$		-1	0	1	2	3	4	5	6	7	8
	2	0	0	0	0	0	0	0	0	0	0
	1	0	0	0	0	0	0	0	0	0	0
	0	0	0	0	0	0	0	0	0	0	0
	-1	0	0	0	0	0	0	0	0	0	0.03
	-2	0.01	0.01	0.01	0.01	0.01	0.01	0.01	0.01	0.03	0.25
	-3	0.10	0.10	0.10	0.10	0.10	0.10	0.10	0.12	0.33	2.03
	-4	0.97	0.97	0.97	0.97	0.97	0.97	0.99	1.18	2.72	7.09
	-5	9.64	9.64	9.64	9.64	9.64	9.64	9.64	9.60	9.50	9.46
	-6	18.3	18.3	18.3	18.3	18.3	18.4	19.3	21.7	12.5	9.76
	-7	18.3	18.3	18.3	18.3	18.4	19.3	21.7	22.8	11.7	9.68
	-8	18.3	18.3	18.3	18.4	19.3	21.7	22.8	14.7	9.98	9.50

*Note:* Calculated as the sum of  $k_D$  from Table 6.11 and  $k_{W,TOT}$  from Table 6.14.

additional field measurements of deposition mass fluxes of chemicals are required to reduce uncertainty in the parameter values recommended here and to evaluate their variability.

LITERATURE CITED

1. Bidleman, T.F. and T. Harner, Sorption to aerosols, in *Handbook of Property Estimation Methods for Chemicals*, R.S. Boethling and D. Mackay, Eds. 2000, CRC Press, Boca Raton, FL, pp. 233–260.

2. Wania, F., J. Axelman, and D. Broman, A review of processes involved in the exchange of persistent organic pollutants across the air–sea interface. *Environmental Pollution*, 1998. **102**(1): 3–23.

3. Cousins, I.T. and D. Mackay, Gas-particle partitioning of organic compounds and its interpretation using relative solubilities. *Environmental Science and Technology*, 2001. **35**(4): 643–647.
4. Pankow, J.F., Review and comparative-analysis of the theories on partitioning between the gas and aerosol particulate phases in the atmosphere. *Atmospheric Environment*, 1987. **21**(11): 2275–2283.
5. Pankow, J.F., An absorption-model of gas-particle partitioning of organic-compounds in the atmosphere. *Atmospheric Environment*, 1994. **28**(2): 185–188.
6. Mackay, D., *Multimedia Environmental Models: The Fugacity Approach*. 2001, Lewis Publishers, Boca Raton, FL, p. 261.
7. Finizio, A., et al., Octanol-air partition coefficient as a predictor of partitioning of semi-volatile organic chemicals to aerosols. *Atmospheric Environment*, 1997. **31**(15): 2289–2296.
8. Götz, C.W., et al., Alternative approaches for modeling gas-particle partitioning of semivolatile organic chemicals: Model development and comparison. *Environmental Science and Technology*, 2007. **41**(4): 1272–1278.
9. Kalberer, M., et al., Identification of polymers as major components of atmospheric organic aerosols. *Science*, 2004. **303**(5664): 1659–1662.
10. Xiao, H. and F. Wania, Is vapor pressure or the octanol-air partition coefficient a better descriptor of the partitioning between gas phase and organic matter? *Atmospheric Environment*, 2003. **37**(20): 2867–2878.
11. Goss, K.U. and R.P. Schwarzenbach, Gas/solid and gas/liquid partitioning of organic compounds: Critical evaluation of the interpretation of equilibrium constants. *Environmental Science & Technology*, 1998. **32**(14): 2025–2032.
12. Goss, K.U., Conceptual model for the adsorption of organic compounds from the gas phase to liquid and solid surfaces. *Environmental Science and Technology*, 1997. **31**(12): 3600–3605.
13. Abraham, M.H., A. Ibrahim, and A.M. Zissimos, Determination of sets of solute descriptors from chromatographic measurements. *Journal of Chromatography A*, 2004. **1037**(1–2): 29–47.
14. Roth, C.M., K.U. Goss, and R.P. Schwarzenbach, Sorption of a diverse set of organic vapors to diesel soot and road tunnel aerosols. *Environmental Science and Technology*, 2005. **39**(17): 6632–6637.
15. Roth, C.M., K.U. Goss, and R.P. Schwarzenbach, Sorption of a diverse set of organic vapors to urban aerosols. *Environmental Science & Technology*, 2005. **39**(17): 6638–6643.
16. Goss, K.U. and R.P. Schwarzenbach, Adsorption of a diverse set of organic vapors on quartz,  $\text{CaCO}_3$ , and  $\alpha\text{-Al}_2\text{O}_3$  at different relative humidities. *Journal of Colloid and Interface Science*, 2002. **252**(1): 31–41.
17. Goss, K.U. and S.J. Eisenreich, Adsorption of VOCs from the gas phase to different minerals and a mineral mixture. *Environmental Science and Technology*, 1996. **30**(7): 2135–2142.
18. Roth, C.M., K.U. Goss, and R.P. Schwarzenbach, Sorption of diverse organic vapors to snow. *Environmental Science and Technology*, 2004. **38**(15): 4078–4084.
19. Seinfeld, J.H. and S.N. Pandis, *Atmospheric Chemistry and Physics: From Air Pollution to Climate Change*. 1998, Wiley, New York, p. 1326.
20. Thibodeaux, L.J., *Environmental Chemodynamics: Movement of Chemicals in Air, Water, and Soil*. 2nd ed. 1996, Wiley, New York, p. 624.

21. Scheringer, M., *Persistence and Spatial Range of Environmental Chemicals: New Ethical and Scientific Concepts for Risk Assessment*. 2002, Wiley-VCH Verlag, Weinheim, p. 308.
22. Jolliet, O. and M. Hauschild, Modeling the influence of intermittent rain events on long-term fate and transport of organic air pollutants. *Environmental Science & Technology*, 2005. **39**(12): 4513–4522.
23. Hertwich, E.G., Intermittent rainfall in dynamic multimedia fate modeling. *Environmental Science and Technology*, 2001. **35**(5): 936–940.
24. Legagneux, L., A. Cabanes, and F. Domine, Measurement of the specific surface area of 176 snow samples using methane adsorption at 77 K. *Journal of Geophysical Research-Atmospheres*, 2002. **107**(D17).
25. Lei, Y.D. and F. Wania, Is rain or snow a more efficient scavenger of organic chemicals? *Atmospheric Environment*, 2004. **38**(22): 3557–3571.
26. Stocker, J., et al., Modeling the effect of snow and ice on the global environmental fate and long-range transport potential of semi-volatile organic compounds. *Environmental Science & Technology*, 2007. **41**(17): 6192–6198.
27. Goss, K.U. and R.P. Schwarzenbach, Empirical prediction of heats of vaporization and heats of adsorption of organic compounds. *Environmental Science & Technology*, 1999. **33**(19): 3390–3393.
28. Roth, C.M., K.U. Goss, and R.P. Schwarzenbach, Adsorption of a diverse set of organic vapors on the bulk water surface. *Journal of Colloid and Interface Science*, 2002. **252**(1): 21–30.
29. Putaud, J.P., et al., European aerosol phenomenology-2: Chemical characteristics of particulate matter at kerbside, urban, rural and background sites in Europe. *Atmospheric Environment*, 2004. **38**(16): 2579–2595.
30. Sehmel, G.A., Particle diffusivities and deposition velocities over a horizontal smooth surface. *Journal of Colloid and Interface Science*, 1971. **37**: 891–906.
31. Sehmel, G.A. and W.H. Hodgson, *A Model for Predicting Dry Deposition of Particles and Gases to Environmental Surfaces*. 1978. Battelle Pacific Northwest Laboratories. Report, Richland, WA.
32. Milford, J.B. and C.I. Davidson, The sizes of particulate trace elements in the atmosphere—a review. *Journal of the Air Pollution Control Association*, 1985. **35**: 1249–1260.
33. Zufall, M.J., et al., Dry deposition of particles to wave surfaces: I. Mathematical modeling. *Atmospheric Environment*, 1999. **33**(26): 4273–4281.
34. Avery, K.R., Literature Search for Atmospheric Humidity Profile Models from the Sea Surface to 1000 Meters. 1972, NOAA Technical Memorandum EDS NODC-1: Silver Spring, MD.
35. Mackay, D., W.Y. Shiu, and K.C. Ma, *Handbook of Physical-Chemical Properties and Environmental Fate for Organic Chemicals*, 2nd ed. 2006, CRC Press, Boca Raton, FL.
36. Fenner, K., et al., Comparing estimates of persistence and long-range transport potential among multimedia models. *Environmental Science and Technology*, 2005. **39**(7): 1932–1942.
37. Davidson, C.I. and Y.L. Wu, Dry deposition of particles and vapors, in *Acidic Precipitation Volume 3*, Lindberg, A.L. and S.A. Norton, Eds. 1990. Springer-Verlag, New York, pp. 103–216.
38. Ruijgrok, W., H. Tieben, and P. Eisinga, The dry deposition of particles to a forest canopy: A comparison of model and experimental results. *Atmospheric Environment*, 1997. **31**(3): 399–415.



39. Brook, J.R., et al., Description and evaluation of a model of deposition velocities for routine estimates of dry deposition over North America. Part II: Review of past measurements and model results. *Atmospheric Environment*, 1999. **33**(30): 5053–5070.
40. Yang, H.H., L.T. Hsieh, and S.K. Cheng, Determination of atmospheric nitrate particulate size distribution and dry deposition velocity for three distinct areas. *Chemosphere*, 2005. **60**(10): 1447–1453.
41. Davidson, C.I., et al., Airborne trace elements in Great Smoky Mountains, Olympic, and Glacier National Parks. *Environmental Science and Technology*, 1985. **19**(1): 27–35.
42. Yi, S., et al., Overall elemental dry deposition velocities measured around Lake Michigan. *Atmospheric Environment*, 2001. **35**(6): 1133–1140.
43. Fang, G.C., et al., Overall dry deposition velocities of trace elements measured at harbor and traffic site in central Taiwan. *Chemosphere*, 2007. **67**(5): 966–974.
44. Fang, G.C., et al., Ambient air particulates, metallic elements, dry deposition and concentrations at Taichung Airport, Taiwan. *Atmospheric Research*, 2007. **84**(3): 280–289.
45. Zufall, M.J., et al., Airborne concentrations and dry deposition fluxes of particulate species to surrogate surfaces deployed in Southern Lake Michigan. *Environmental Science and Technology*, 1998. **32**(11): 1623–1628.
46. Vardar, N., M. Odabasi, and T. Holsen, Particulate dry deposition and overall deposition velocities of polycyclic aromatic hydrocarbons. *Journal of Environmental Engineering–ASCE*, 2002. **128**(3): 269–274.
47. Sharma, M. and E. McBean, Atmospheric PAH deposition: Deposition velocities and washout ratios. *Journal of Environmental Engineering–ASCE*, 2002. **128**(2): 186–195.
48. McVeety, B.D. and R.A. Hites, Atmospheric deposition of PAHs to water surfaces: A mass balance approach. *Atmospheric Environment Part a—General Topics*, 1988. **22**(2): 511–536.
49. Franz, T., S. Eisenreich, and T. Holsen, Dry deposition of particulate polychlorinated biphenyls and polycyclic aromatic hydrocarbons to Lake Michigan. *Environmental Science and Technology*, 1998. **32**(23): 3681–3688.
50. Tasdemir, Y., et al., Dry deposition fluxes and velocities of polychlorinated biphenyls (PCBs) associated with particles. *Atmospheric Environment*, 2004. **38**(16): 2447–2456.
51. Bozlaker, A., M. Odabasi, and A. Muezzinoglu, Dry deposition and soil-air gas exchange of polychlorinated biphenyls (PCBs) in an industrial area. *Environmental Pollution*, 2008. **156**(3): 784–793.
52. Sheu, H.L., et al., Dry deposition of polycyclic aromatic hydrocarbons in ambient air. *Journal of Environmental Engineering*, 1996. **112**(12): 1101–1109.
53. Odabasi, M., et al., Measurement of dry deposition and air-water exchange of polycyclic aromatic hydrocarbons with the water surface sampler. *Environmental Science and Technology*, 1999. **33**(3): 426–434.
54. Poster, D. and J. Baker, Mechanisms of atmospheric wet deposition of chemical contaminants, in *Atmospheric Deposition of Contaminants to the Great Lakes and Coastal Waters: Proceedings from a Session at SETAC's 15th Annual Meeting*, J. Baker, Ed. 1997, SETAC Press, Pensacola, FL.
55. Franz, T., D. Gregor, and S. Eisenreich, Snow deposition of atmospheric semivolatile organic chemicals, in *Atmospheric Deposition of Contaminants to the Great Lakes and Coastal Waters*, J. Baker, Ed. 1997, SETAC Press, Pensacola, FL.
56. Kasper-Giebl, A., M.F. Kalina, and H. Puxbaum, Scavenging ratios for sulfate, ammonium and nitrate determined at Mt. Sonnblick (3106 m asl). *Atmospheric Environment*, 1999. **33**(6): 895–906.
57. Schnoor, J., *Environmental Modeling*. 1996. Wiley Interscience, New York.

58. Franz, T.P. and S.J. Eisenreich, Snow scavenging of polychlorinated biphenyls and polycyclic aromatic hydrocarbons in Minnesota. *Environmental Science and Technology*, 1998. **32**(12): 1771–1778.
59. Wania, F., D. Mackay, and J.T. Hoff, The importance of snow scavenging of polychlorinated biphenyl and polycyclic aromatic hydrocarbon vapors. *Environmental Science and Technology*, 1999. **33**(1): 195–197.
60. Agrell, C., et al., PCB congeners in precipitation, wash out ratios and depositional fluxes within the Baltic Sea region, Europe. *Atmospheric Environment*, 2002. **36**(2): 371–383.
61. Zufall, M.J., M.H. Bergin, and C.I. Davidson, Effects of non-equilibrium hygroscopic growth of  $(\text{NH}_4)_2\text{SO}_4$  on dry deposition to water surfaces. *Environmental Science and Technology*, 1998. **32**(5): 584–590.

## FURTHER READING

- Boethling, R.S. and D. Mackay, Eds. *Handbook of Property Estimation Methods for Chemicals*, 2000, CRC Press, Boca Raton, FL.
- Schnoor, J., *Environmental Modeling*. 1996. Wiley Interscience, New York.
- Seinfeld, J.H. and S.N. Pandis, *Atmospheric Chemistry and Physics: From Air Pollution to Climate Change*. 1998. Wiley, New York, p. 1326.
- Thibodeaux, L.J., *Environmental Chemodynamics: Movement of Chemicals in Air, Water, and Soil*. 2nd ed. 1996. Wiley, New York, p. 624.